Silver(I)-Selective Electrodes Based on Rare Earth Element Double-Decker Porphyrins

Narender Kumar Joon[a], Jonathan E. Barnsley[b], Ruiyu Ding[c], Sunri Lee[d], Rose-Marie Latonen[a], Johan Bobacka[a], Keith C. Gordon[c], Takuji Ogawa[d], Grzegorz Lisak[c,e,*]

[a] *Johan Gadolin Process Chemistry Centre, Laboratory of Analytical Chemistry, Åbo Akademi University, Biskopsgatan 8, 20500 Åbo-Turku, Finland*

[b] *MacDiarmid Institute for Advanced Materials and Nanotechnology, Chemistry Department, University of Otago, Dunedin, New Zealand*

[c] *College of Engineering, School of Civil and Environmental Engineering, Nanyang Technological University, 50 Nanyang Avenue, Singapore 639798, Singapore*

[d] *Department of Chemistry, Graduate School of Science, Osaka University, 1-1 Machikaneyama-cho, Toyonaka, Osaka 560-0043, Japan*

[e] *Nanyang Environment and Water Research Institute, Residues and Resource Reclamation Center, 1 Cleantech Loop, CleanTech, Singapore 637141, Singapore*

Corresponding author: g.lisak@ntu.edu.sg

Abstract

Various double decker porphyrins accommodating rare earth elements (Sm, Tb, Y) were investigated as ionophores in potentiometric ion sensors. The studied ion-selective electrodes based on double decker porphyrins were primarily selective to Ag^+ ions. The experimentally derived selectivity coefficients were compared to theoretical predictions based on density functional theory (DFT) calculations of the metal-binding energies (ΔE) of double decker porphyrin-metal ion complexes. Although DFT calculations were performed *in vacuo*, without taking into account ion-solvent and ion-membrane interactions, this computational approach showed relatively good correlation with the experimentally observed selectivity patterns of the ion-selective electrodes. Thus, DFT calculations were found to be a useful predictive tool when designing new ionophores for ion-selective electrodes.

Keywords: Double decker porphyrins, rare earth metals, silver selective electrodes, potentiometric sensors, DFT calculations

1. Introduction

Potentiometric ion sensors are constantly investigated for the determination of environmentally and clinically relevant analytes. Analysis in such a wide range of samples pose challenges in the development of a universal ion-selective electrode (ISE) that would operate at a wide concentration range (molar to submicromolar), be selective to all interfering ions and be characterized with pH independent response. Instead, individual ISEs are usually being customized for specific applications and specific sample types. This triggered the research towards development and optimization of high performance ionophores suitable for sensitive determination of analytes in various samples. Bühlmann, Bakker and Pretsch recognized and summarized a wide range of ionophores, which covered a broad spectrum of synthetic organic molecules, e.g. derivatives of amides, crown ethers, calixarenes and single ring porphyrins [1–3].

Porphyrins are studied extensively for their strong complexing properties, stability and catalytic behavior in various fields such as catalysis, sensors, biomedicine and photonics. Their sensor applications cover chromatography, pre-concentration techniques, spectroscopy and electroanalysis. Porphyrins have strong affinity to certain ions and are used as ionophores in ISEs and optodes [2,4–7]. Owing to the electron-rich interior cavities of porphyrins, they have the ability to selectively bind metal ions, forming metal-porphyrin complexes. This metal-ion binding characteristic of porphyrins has been utilized for the development of various cation-selective ISEs [5,8–14].

In this work newly synthesized double-decker porphyrins, namely, Sm^{III}(TPP)(TPPH); Y^{III}(TPP)(TPPH); $Sm^{III}(TPP)_2$; $Tb^{III}(TPP)_2$; Tb^{III}(C8P) (C8PH) and Tb^{III}((p-OMe)PP) (p-OMe)PPH) (TPP, tetraphenylporphyrinato(2-); C8P, di(*n*-octyl)porphyrinato(2-); (p-OMe)PP, tetrakis(4-methoxyphenyl)porphyrinato(2-)) were studied as ionophores in ion-selective membranes (ISMs). The experimentally derived selectivity patterns were compared to theoretical predictions based on DFT calculations.

2. Experimental Section

2.1. Reagents and materials

Cadmium nitrate tetrahydrate, $Cd(NO_3)_2 \cdot 4H_2O$; calcium nitrate tetrahydrate, $Ca(NO_3)_2 \cdot 4H_2O$; cobalt nitrate hexahydrate, $Co(NO_3)_2 \cdot 6H_2O$ (purity ≥ 97%); magnesium nitrate hexahydrate, $Mg(NO_3)_2 \cdot 6H_2O$; nickel nitrate hexahydrate, $Ni(NO_3)_2 \cdot 6H_2O$; strontium nitrate, $Sr(NO_3)_2$; potassium nitrate, KNO_3; sodium hydroxide NaOH and sodium nitrate, $NaNO_3$ were purchased from Merck (Darmstadt, Germany). Tridodecylmethylammonium chloride, TDMACl; poly(sodium 4-styrenesulfonate), NaPSS (Mw ~70,000); 3,4-ethylenedioxythiophene, EDOT (>97%); nitric acid HNO_3 and copper nitrate trihydrate, $Cu(NO_3)_2 \cdot 3H_2O$ were purchased from Sigma-Aldrich (Steinheim, Germany). Potassium tetrakis(4-chlorophenyl)borate (KTClPB); 2-nitrophenyl octyl ether, o-NPOE; poly(vinyl chloride) of high molecular weight, PVC, tetrahydrofuran, THF and lead(II) nitrate $Pb(NO_3)_2$ were purchased from Fluka (Buchs, Switzerland). Silver (I) nitrate, $AgNO_3$ was purchased from J.T. Baker (Central Valley, USA) while barium nitrate, BaN_2O_6 was purchased from Acros organics (Geel, Belgium). All nitrate based salts were with minimum 99% purity unless specified otherwise. The aqueous solutions were freshly prepared with deionized water (18.2 MΩ cm resistivity) obtained from an ELGA purelab ultra water system (High Wycombe. United Kingdom).

Double decker porphyrins shown in **Figure 1** were synthetized by identical procedure with the reported method[15] identified by elemental analyses and are studied as ionophores in ISEs.

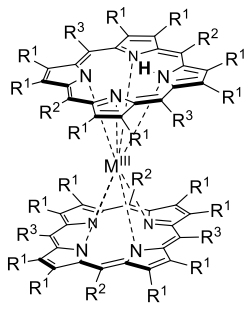

Sm^{III}(TPP)(TPPH):M=Sm, R^1=H, R^2=R^3=C_6H_5-
Y^{III}(TPP)(TPPH):M=Y, R^1=H, R^2=R^3=C_6H_5-
Tb^{III}((p-OMe)PP)(p-OMe)PPH): M=Tb, R^1=H, R^2=R^3=4-$CH_3OC_6H_4$-
Tb^{III}(C8P)(C8PH): M=Tb, R^1=R^2=H, R^3=*n*-C_8H_{17}-

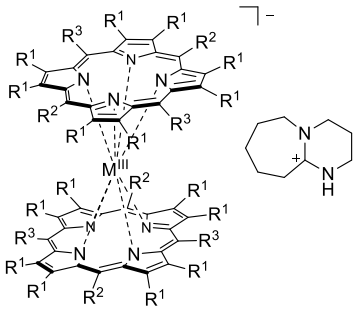

$Sm^{III}(TPP)_2$:M=Sm, R^1=H, R^2=R^3=C_6H_5-
$Tb^{III}(TPP)_2$:M=Tb, R^1=H, R^2=R^3=C_6H_5-

Figure 1. Double decker porphyrins investigated as ionophores in ISEs.

2.2. Electrodes preparation, selectivity and pH sensitivity measurements

Glassy carbon electrodes (GC) enclosed in a teflon body were cleaned by polishing using 0.3 μm Al_2O_3, followed by vigorous washing with deionized water, subsequent washing with 99.5% ethanol and finalized with washing using deionized water. The electrodes were then left for one hour to dry in air. An Autolab PGSTAT 30 (Metrohm) controlled by a General Purpose Electrochemical System (GPES) software was used to electrosynthesize poly(3.4-ethylenedioxythiophene) (PEDOT) on previously cleaned glassy carbon electrodes. PEDOT was electrodeposited and doped with polystyrene sulfonate (PSS^-) by electropolymerization from a solution of 0.01 mol dm^{-3} 3.4-ethylenedioxythiophene (EDOT) in 0.1 mol dm^{-3} NaPSS. The PEDOT(PSS) electropolymerization was performed in a three electrodes system consisting of the GC as working electrode (WE), GC rod as counter electrode (CE) and a single junction Ag/AgCl/3M KCl as reference electrode (RE) by applying a current density of 0.2 mA cm^{-2} to the working electrode for 714 s [7,16,17]. After electropolymerization, the GC/PEDOT(PSS) electrodes were rinsed with deionized water and left in air for 2 hours to dry, followed by drop casting of the ion-selective membrane from appropriate membrane cocktails on top of GC/PEDOT(PSS). The membrane composition consisted of 100 mg dry mass of membrane components dissolved in 1 ml of THF. Each ISM contained (by weight) 1% ionophore (double-decker porphyrin), 0.2% KTClPB, 66% o-NPOE and 32.8% PVC [7]. Total 60 μl of cocktail was used to form each ISM. Subsequently, the electrodes were left overnight in air for residual solvent evaporation. For each double-decker porphyrin-based membrane, three ISEs were prepared (n= 3).

All potentiometric measurements were performed using EMF16 Interface (Lawson Labs Inc., USA) to follow the potential (*E*) of potentiometric cell consisting of indicator electrodes (double-decker porphyrin-based ISEs) and a double-junction reference electrode, Ag/AgCl/3 mol dm^{-3} KCl/10^{-1} LiAc. For all electrodes, the unbiased selectivity coefficients, for primary over interfering ions were determined by the separate solution method (SSM) [18,19]. For that, newly prepared and unconditioned ISEs were used [7]. The selectivity measurements were done by registering the potential when decreasing the ion activities in the standard solution, from ~10^{-1} to 10^{-3} mol dm^{-3}. Two Metrohm Dosino 700 instruments equipped with burets of 50 mL capacity (Herisau, Switzerland) were utilized for the automatic dilutions of stock solutions. The pumps were programmed to dilute the sample solution with freshly deionized water (18.2 MΩ cm) every

5 min. All measurements were carried out in 100 ml glass beakers. All the solutions were prepared from nitrate salts of the cations studied. The uncertainties (SD) of selectivity coefficients were obtained from the measurement done with three identical electrodes. The potentiometric sensitivity to Ag^+ was conducted on ISEs that were conditioned in 10^{-3} mol dm^{-3} $AgNO_3$ for 24 hours. The potential was recorded from $\sim 10^{-1}$ to 10^{-8} mol dm^{-3} of $AgNO_3$. To investigate the effect of pH on the potentiometric response of ISEs, electrodes based on all porphyrins Y^{III}(TPP)(TPPH), Sm^{III}(TPP)(TPPH), $Tb^{III}(TPP)_2$, $Tb^{III}(C8P)^2H$ and T(p-OMe)PP_2TbH) were freshly prepared. The potential stability of the electrodes, at various pH (pH 2 – 10), was analyzed in 50 ml of 0.1 mol dm^{-3} KNO_3. The potential was analyzed for ca. 5 minutes for every pH change, and then the pH was adjusted with small aliquots of the NaOH or HNO_3. Concentrated NaOH and HNO_3 were used, to change the pH of 0.1 mol dm^{-3} KNO_3 solution; and to avoid significant change in the concentration of KNO_3. The potentials were measured with EMF16 interface and a double junction reference electrode (Ag/AgCl/3 mol dm^{-3} KCl/10^{-1} LiAc) was used as reference electrode. The activities were calculated form Debye-Hückel equation. All experiments were carried out at room temperature (22 ± 3°C).

2.3. Computational Methods

Geometry and vibrational calculations were generated using the Gaussian 09W program package. The ωB97XD functional was used with the Stuttgart RSC 1997 [20] basis set and associated ECP applied for yttrium atoms, while the LANL2DZ [21–23] basis set and associated ECP was used for Ag^+, Ca^{2+}, Cd^{2+}, K^+, Na^+, Ni^{2+}, Mg^{2+}, Pb^{2+}, Sr^{2+} and Zn^{2+} atoms. For all other atoms, the 6-31G(d,p) [24,25] basis was used. All calculations were carried out *in vacuo*.[26] This particular computational approach was used as it has been observed to give useful structures and energy approximations by Ogawa *et al.* [15] and Kitagawa *et al.* [27] for lanthanide double decker porphyrins. Following the optimization of each structure, frequency calculations were run and only structures with no negative frequencies, thus located in an energy minima, were used. The energy of the optimized structure was used to calculate metal-binding energies (ΔE) for the binding of each ion in the YTPP double decker porphyrin. This was achieved using the following chemical equations:

$YTPP^- + M(NO_3)_n \rightarrow M\text{-}YTPP^{(-1+n)} + (NO_3^-)_n$ **Equation 1**

$\Delta E = (E_{M\text{-}YTPP}^{(-1+n)} + E_{(NO_3^-)n}) - (E_{YTPP^-} + E_{M(NO_3)n})$ **Equation 2**

Distortion energies were calculated by the removal of M from the M-YTPP$^{(-1+n)}$ structures, which was then run using a single point calculation:

$E_{distortion} = YTPP_{Mremoved}^- - YTPP_{opt.}^-$ **Equation 3**

Note that Co^{2+} and Cu^{2+} were not calculated as the ground states are typically not of singlet nature, and necessitate the use of unrestricted DFT methods.

3. Results and Discussion

3.1. Anion and cation sensitivity of double decker porphyrin based ISEs.

Recently, we have investigated porphyrin dimer-based systems to be applied as ionophores in ISEs for the detection of both anions and cations [7]. The porphyrin dimers consisted of both free base and metalloporphyrin units (mix sensitivity porphyrin units, anion- and cation-sensitive). Thus, the dualism of sensitivity to either cations or anions came from the fact that the porphyrin dimers were acting as neutral ionophores and the initial response toward primary ion was dependent on the lipophilic ion additive in the ion-selective membrane (ISM) [7]. In the present study, we investigate a different type of advanced porphyrin systems comprised of two porphyrin rings linked with one central atom (double-decker porphyrins) as ionophores in ISEs. Previously, such porphyrin systems were identified with cation binding [28]. Considering the molecular structure of the double decker porphyrins (central atom shared between two porphyrin rings), the porphyrin systems were investigated here for their cationic and anionic sensitivity. Yet again, double-decker porphyrins were treated as neutral ionophores and by changing the ionic additive in the ISM, the anionic and cationic sensitivity and selectivity were investigated. Thus, ISMs containing double-decker porphyrins and TDMACl (lipophilic $TDMA^+$ cation) were investigated for their anionic sensitivity (supporting information, Table S1), while ISMs containing double-decker porphyrins and KTClPB (lipophilic $TClPB^-$ anion) were investigated for their cationic sensitivity. Additionally, the selectivity of all double-decker porphyrin-based sensors was investigated and compared to ISEs without any porphyrins in ISM, containing only TDMACl or KTClPB.

The anion-selectivity of $Sm^{III}(TPP)_2$, $Sm^{III}(TPP)(TPPH)$, $Y^{III}(TPP)(TPPH)$, $Tb^{III}(TPP)_2$, $Tb^{III}(C8P)_2H$ and $T(p\text{-}OMe)PP_2Tb^{III}H$ based ISM electrodes were compared to the TDMACl-based ISM. It was found (supporting information, Table S1) that the selectivity of the TDMACl-based ISM was comparable to all double-decker porphyrins based ISMs. In general, metalloporphyrins are sensitive to anions but in double-decker porphyrin the central atom is shielded by the two porphyrin rings. This limits the availability of the central atom to form the complex with an anion making double-decker porphyrins non-selective for anions. This can be visually represented with a total electron density map generated using DFT for the Y-based double decker porphyrin (**Figure 2**). In this case, the approach of the anion towards the central metallic atom is electronically and sterically hindered. Note that this is true with or without the hydrogenated amine unit, e.g. $Y(TPP)_2$ and Y(TPP)(TPPH). Approach of an ion into either a porphyrin- or aryl cleft may be possible. These binding sites have been identified previously by Ikeda et. al who published ^{1}HNMR evidence suggesting the porphyrin cleft becomes occupied by Ag^+ [28]. With only access to porphyrin- or aryl clefts it would be expected that cations will interact with these materials, while anions would not. This would explain why the double-decker porphyrins do not significantly influence the anion-selectivity of the ISMs studied here (supporting information, Table S1).

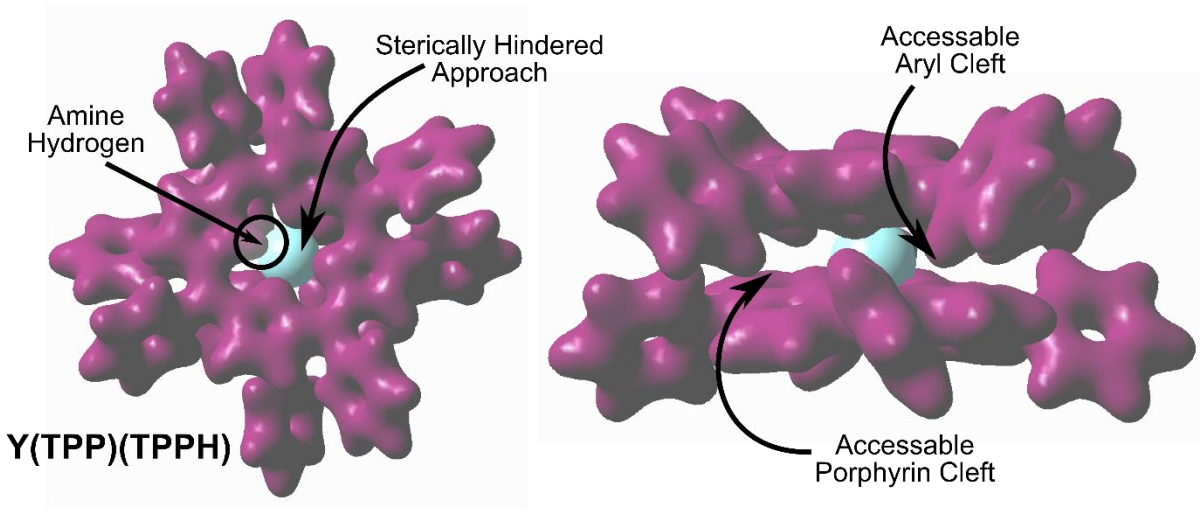

Figure 2. A total density plot of Y(TPP)(TPPH) drawn in GaussView 5 with standard visual parameters (density = 0.05 and isovalue 0.02).

3.2. Selectivity of double decker porphyrin based ISEs.

Based on the results and considerations presented above, the double-decker porphyrins were employed further for cation-selective ISEs. The selectivity measurements applying separate solution method (SSM) show that the double-decker porphyrins are selective to Ag^+ ions over other interfering ions, as summarized in **Tables 1** and **2**. The selectivity of all double-decker porphyrin-based sensors to Ag^+ were much better than the ones obtained for the KTClPB-based sensors without ionophore (Table 1), indicating that the KTClPB plays a role of ionic additive while double-decker porphyrins are responsible for the overall selectivity of the ISM. The selectivity coefficients for Ag^+ over interfering ions of ISEs with terbium-based ionophores are shown in Table 1. The selectivity to Ag^+ over most of the interfering ions were significantly better for the $Tb^{III}(TPP)_2$ ionophore than for the T(p-OMe)$PP_2Tb^{III}H$ and $Tb^{III}(C8P)_2H$ ionophores. Among these three ionophores, the $Tb^{III}(C8P)_2H$ ionophore having aliphatic substituents (Figure 1) gave the lowest selectivity to Ag^+(Table 1). As identified by Ikeda et al., cation binding occurs either in the porphyrin or aryl cleft. The results obtained here indicate that aryl substituents, particularly the phenyl substituent in $Tb^{III}(TPP)_2$, improve the selectivity for Ag^+ ions, compared to the lower selectivity obtained with $Tb^{III}(C8P)_2H$ having aliphatic substituents. Thus, the moiety attached to the double-decker porphyrin have a large impact on its cation binding properties. For comparison, it may be noted that [2.2.2]*p,p,p*-cyclophane showed relatively high selectivity to Ag^+ based on interactions between Ag^+ and phenyl groups [29]. Furthermore, the [2.2.2]*p,p,p*-cyclophane was much more selective to Ag^+ as compared with the closely related [2.2.2]*m,p,p*-cyclophane [29].

The selectivity coefficients for Ag^+ over interfering ions of ISEs with samarium and yttrium-based double-decker porphyrin ionophores are shown in Table 2. The $Sm^{III}(TPP)(TPPH)$, which is the protonated double-decker porphyrin, exhibits better selectivity towards Ag^+ over other interfering ions than $Sm^{III}(TPP)_2$-based sensors. On the contrary, $Y^{III}(TPP)_2$ based sensors exhibit similar selectivity towards Ag^+ as the sensors that contained $Y^{III}(TPP)(TPPH)$ as ionophore. It is expected that the additional proton in protonated double decker porphyrins ($Sm^{III}(TPP)(TPPH)$ and $Y^{III}(TPP)(TPPH)$) would slightly alter the orientation of the porphyrin rings compared to orientation of the non-protonated double decker porphyrins ($Sm^{III}(TPP)_2$ and $Y^{III}(TPP)_2$). Such orientation change, however, cannot be attributed to discernible difference in metal-double decker porphyrin affinity (more deliberated in subsequent chapters).

To summarize, all double-decker porphyrin-based ISEs were selective to Ag^+. Moreover, all double-decker porphyrin-based ISEs followed similar selectivity pattern for Ag^+ over other interfering ions, namely the most interfering ions were found to be K^+, Cu^{2+}, Pb^{2+} while the least interfering ions were found to be Zn^{2+}, Ca^{2+}, Mg^{2+}. Similarly, the selectivity of the ISEs to Ag^+ over monovalent interfering ions followed the same pattern, namely $Ag^+ > K^+ > Na^+$. On the other hand, the selectivity of ISEs to Ag^+ over the rest of interfering ions (intermediate selectivity) did not follow a specific selectivity pattern and the differences in the selectivity coefficients were relatively small for these ions. The changes were primarily attributed to chemical modifications of double decker porphyrins and their subsequent ionophore-ion interactions. In some cases the slope for divalent interfering ions was sub-Nernstian (<15 mV dec^{-1}), e.g 10.8 ± 0.1 mV dec–1 for Ni^{2+} and 2.8 ± 0.2 mV dec^{-1}, 9.0 ± 0.3 mV dec^{-1}, 4.1 ± 0.8 mV dec^{-1}, 14.2 ± 1.9 mV dec^{-1}, 14.9 ± 1.8 mV dec^{-1} for Sr^{2+} calibrations using Tb^{III}(C8P)2H, T(p-OMe)PP2Tb^{III}H, Sm^{III}(TPP)(TPPH), $Y^{III}(TPP)_2$ and Y^{III}(TPP)(TPPH) based ISEs, respectively. This indicates that the selectivity measurements for Ag+ over these interfering ions (showing intermediate selectivity) have a high uncertainty.

The potentiometric selectivity coefficients of the double decker porphyrins studied in this work can be compared with those of similar ionophores published earlier. Ardakani et al. showed an Ag^+-selective ISEs based on meso-tetraphenlyporphyrin. The most interfering ions reported were Na^+ and Cu^{2+} whereas Co^{2+} and Sr^{2+} showed low interference[30]. Similarly, Zhang et al. used corroles (ring contracted analogues of porphyrins) as an electroactive material for the silver selective ISEs. The reported selectivity coefficients were in the range of –3.21 to –4.67. In Zhang's paper, the most interfering ions reported were Cu^{2+} and K^+ whereas the least interfering ions were Ca^{2+} and Zn^{2+}[31]. Vlascici et al. also reported two different silver selective porphyrins, i.e. (5,10,15,20-tetrakis(3,4-dimetoxyphenyl) porphyrin and 5,10,15,20-tetrakis(3-hydroxyphenyl) porphyrin). In both the porphyrins, Zn^{2+} was reported as least interfering while K^+ and Cu^{2+} showed the highest interference[32]. Lisak et al. also reported the selectivities of porphyrins dimers based ISEs, where the most interfering cations reported were K^+, Cu^{2+} and Pb^{2+} and least interfering cations were Mg^{2+}, Zn^{2+} and Ca^{2+} [7]. A similar pattern is observed for most of the double decker porphyrin-based ISEs reported in this work, with some of the double decker porphyrin-based ISEs studied exhibiting superior selectivity to Ag^+ (Tables 1 and 2).

Table 1. Selectivity coefficients for Ag^+ over interfering ions for $Tb(TPP)_2$, $Tb(C8P)_2H$ and $Tb(p\text{-}oMe)PP_2TbH$ used as ionophores in Ag^+-ISEs.

Interfering ion / *j*	KTClPB		Tb(TPP)2		Tb(C8P)2H		Tb(p-oMe)PP2TbH	
	slope	$logK^{pot}_{Ag^+,j}$	slope	$logK^{pot}_{Ag^+,j}$	slope	$logK^{pot}_{Ag^+,j}$	slope	$logK^{pot}_{Ag^+,j}$.
Mg^{2+}	15.7 ± 1.2	–5.91 ± 0.55	24.9 ± 0.8	–8.61 ± 0.03	17.2 ± 1.4	–5.79 ± 0.10	19.5 ± 0.9	–8.46 ± 0.45
Ca^{2+}	26.8 ± 2.7	–3.48 ± 0.26	21.4 ± 0.5	–8.31 ± 0.12	1.2 ± 0.5	–5.38 ± 0.27	13.9 ± 1.7	–8.02 ± 0.08
Co^{2+}	26.2 ± 0.2	–3.73 ± 0.09	24.7 ± 1.7	–7.84 ± 0.11	31.4 ± 4.9	–4.05 ± 0.04	23.0 ± 0.2	–5.21 ± 0.40
Zn^{2+}	24.1 ± 0.1	–3.87 ± 0.14	23.5 ± 0.7	–8.61 ± 0.28	11.4 ± 1.2	–5.14 ± 0.06	19.7 ± 1.0	–6.34 ± 0.06
Cu^{2+}	25.1 ± 2.0	–2.87 ± 0.06	31.3 ± 2.1	–4.93 ± 0.04	27.7 ± 0.2	–3.64 ± 0.05	29.4 ± 0.5	–4.98 ± 0.33
Ni^{2+}	29.6 ± 0.2	–4.02 ± 0.06	30.4 ± 2.7	–7.11 ± 0.22	10.8 ± 0.1	–4.92 ± 0.08	22.0 ± 1.3	–5.62 ± 0.01
Pb^{2+}	20.4 ± 2.2	–2.67 ± 0.04	30.6 ± 2.6	–5.19 ± 0.11	29.4 ± 0.1	–3.51 ± 0.10	31.6 ± 0.9	–4.46 ± 0.04
Cd^{2+}	26.4 ± 0.7	–4.17 ± 0.31	21.5 ± 4.8	–8.30 ± 0.27	27.6 ± 3.3	–4.25 ± 0.16	19.5 ± 1.2	–5.85 ± 0.21
Sr^{2+}	28.8 ± 0.1	–3.48 ± 0.42	19.3 ± 0.4	–7.43 ± 0.03	2.8 ± 0.2	–4.98 ± 0.23	9.0 ± 0.3	–5.69 ± 0.03
Na^+	59.5 ± 1.1	–2.58 ± 0.26	45.1 ± 0.6	–6.45 ± 0.07	10.6 ± 3.7	–4.67 ± 0.04	30.5 ± 2.6	–6.00 ± 0.06
K^+	59.2 ± 0.6	–2.28 ± 0.16	52.3 ± 0.7	–3.35 ± 0.03	19.9 ± 1.5	–4.12 ± 0.09	32.6 ± 1.9	–4.02 ± 0.04
Ag^+	53.0 ± 2.3	0	50.1± 1.6	0	53.5 ± 2.4	0	50.4 ± 1.7	0

Table 2. Selectivity coefficients for Ag^+ over interfering ions for $Sm(TPP)_2$, Sm(TPP)(TPPH), $Y(TPP)_2$ and Y(TPP)(TPPH) used as ionophores in Ag^+-ISEs.

Interfering ion / *j*	$Sm(TPP)_2$		Sm(TPP)(TPPH)		$Y(TPP)_2$		Y(TPP)(TPPH)	
	slope	$logK^{pot}_{Ag^+,j}$	slope	$logK^{pot}_{Ag^+,j}$	slope	$logK^{pot}_{Ag^+,j}$	slope	$logK^{pot}_{Ag^+,j}$
Mg^{2+}	20.9 ± 1.6	–7.72 ± 0.12	19.1 ± 0.1	–9.33 ± 0.32	17.2 ± 1.0	-8.30 ± 0.13	12.5 ± 0.6	–8.00 ± 0.06
Ca^{2+}	19.9 ± 0.8	–7.49 ± 0.18	18.1 ± 1.0	–9.74 ± 0.25	15.8 ± 1.3	-7.91 ± 0.09	22.0 ± 1.6	–7.48 ± 0.02
Co^{2+}	29.3 ± 2.6	–6.18 ± 0.37	31.5 ± 2.7	–8.11 ± 0.30	35.4 ± 0.4	-5.78 ± 0.16	29.4 ± 1.2	–5.66 ± 0.35
Zn^{2+}	32.4 ± 2.9	–6.44 ± 0.31	24.1 ± 0.5	–8.30 ± 0.41	24.1 ± 0.2	-7.09 ± 0.10	31.4 ± 2.6	–6.36 ± 0.21
Cu^{2+}	27.1 ± 2.7	–4.02 ± 0.15	28.2 ± 0.6	–4.75 ± 0.10	29.7 ± 1.3	-4.34 ± 0.06	29.4 ± 1.4	–4.85 ± 0.03
Ni^{2+}	24.3 ± 0.9	–5.14 ± 0.11	26.2 ± 0.9	–7.24 ± 0.31	28.4 ± 1.6	-5.62 ± 0.20	26.9 ± 3.0	–5.91 ± 0.24
Pb^{2+}	30.3 ± 1.0	–3.36 ± 0.10	27.7 ± 1.3	–5.00 ± 0.22	28.6 ± 0.8	-4.00 ± 0.14	31.0 ± 2.6	–4.78 ± 0.16
Cd^{2+}	34.1 ± 2.0	–5.54 ± 0.22	21.0 ± 0.2	–5.72 ± 0.21	27.0 ± 1.4	-5.81 ± 0.21	28.6 ± 2.8	–5.44 ± 0.12
Sr^{2+}	27.3 ± 4.5	–5.85 ± 0.23	4.1 ± 0.8	–7.60 ± 0.24	14.2 ± 1.9	-6.00 ± 0.02	14.9 ± 1.8	–6.20 ± 0.29
Na^+	48.4 ± 0.3	–5.27 ± 0.10	43.6 ± 1.5	–7.53 ± 0.30	41.5 ± 2.1	-6.62 ± 0.08	40.3 ± 5.0	–5.69 ± 0.34
K^+	54.4 ± 3.1	–2.78 ± 0.10	50.0 ± 0.9	–4.59 ± 0.19	40.8 ± 1.8	-3.96 ± 0.19	42.7 ± 3.5	–4.45 ± 0.08
Ag^+	53.7 ± 2.8	0	51.4 ± 1.8	0	51.3 ± 1.5	0	55.0 ± 1.2	0

3.3. Potentiometric response of silver-selective ISEs.

The potentiometric responses of double-decker porphyrin based ISEs to Ag^+ were investigated between $10^{-1.1}$ and $10^{-8.0}$ mol dm^{-3} $AgNO_3$ after 24 h conditioning of the ISEs in $10^{-3.0}$ mol dm^{-3} $AgNO_3$. The results are presented in **Figure 3**, where all ISEs exhibit cationic response to the main ion. The calculated slopes (between $10^{-1.1}$ and $10^{-4.0}$ mol dm^{-3} $AgNO_3$) were 43.3, 56.5, 43.0, 51.0, 46.3, 45.0 and 45.7 mV dec^{-1} for $Sm^{III}(TPP)(TPPH)$, $Y^{III}(TPP)(TPPH)$, $Y^{III}(TPP)_2$, $Sm^{III}(TPP)_2$, $Tb^{III}(TPP)_2$, $T(p\text{-}OMe)PP_2Tb^{III}H$ and $Tb^{III}(C8P)_2H$ based ISEs, respectively. The low

detection limits for all invested electrodes were between $10^{-5.0}$ and $10^{-5.1}$ mol $dm^{-3}AgNO_3$. In general, closer to Nernstian slopes (above 50 mV dec^{-1}) were obtained during the selectivity measurements when all the ISEs were first time in contact with the silver ion. Only Y^{III}(TPP)(TPPH) based electrode had close to Nernstian response after 24 h conditioning in $10^{-3.0}$ mol $dm^{-3}AgNO_3$.

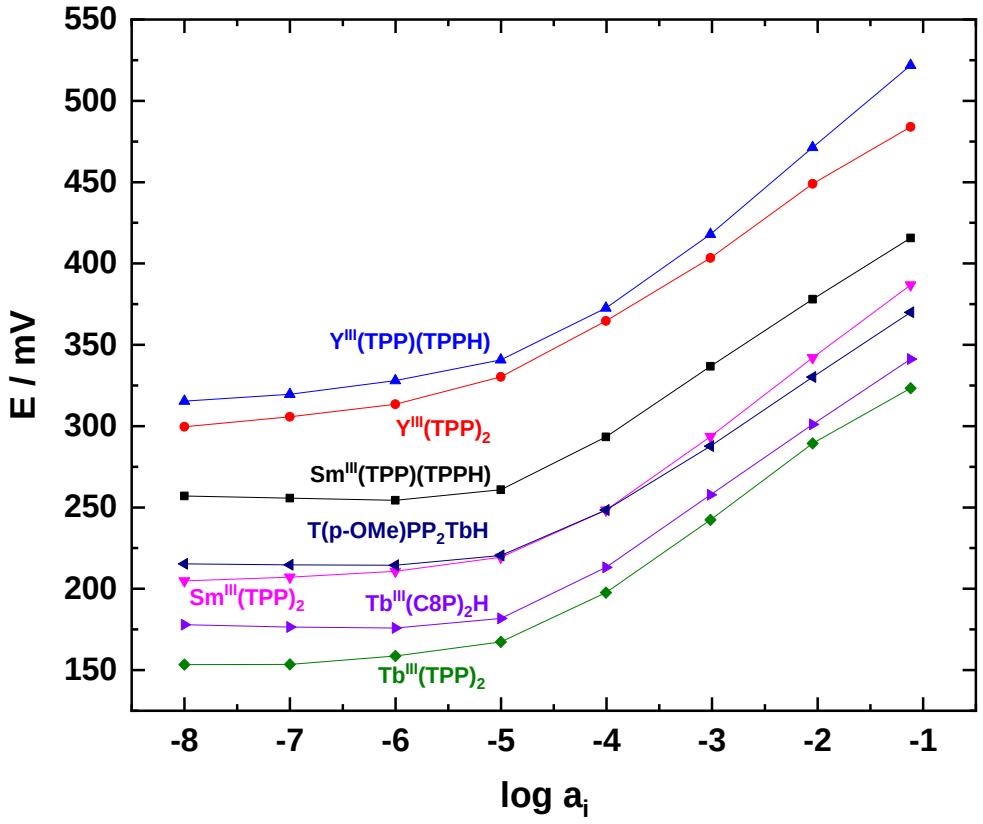

Figure 3. Potentiometric response of Ag^+-ISEs based on double decker porphyrins as ionophores measured in the activity range from $10^{-1.1}$ to $10^{-8.0}$ mol $dm^{-3}AgNO_3$ after 24 h conditioning of the ISEs in $10^{-3.0}$ mol $dm^{-3}AgNO_3$.

Figure 4 shows pH sensitivity of porphyrin based ISEs in the presence of 0.1 mol dm^{-3} KNO_3. The pH of the 0.1 mol dm^{-3} KNO_3 was determined to be approx. 4.9. At acidic pH (pH 2–5), the double decker porphyrin based ISEs showed sensitivity towards the proton. Though, $Tb^{III}(C8P)_2H$

showed a small drop in potential in the pH range of 6 to 10, other porphyrins retained pH independent response at the neutral to alkaline pH, resulting into stable potential in the pH range of 5 to 10. The pH independent ISEs response in the pH range of 5 to 10 should assure interference free response of silver(I)-ISEs.

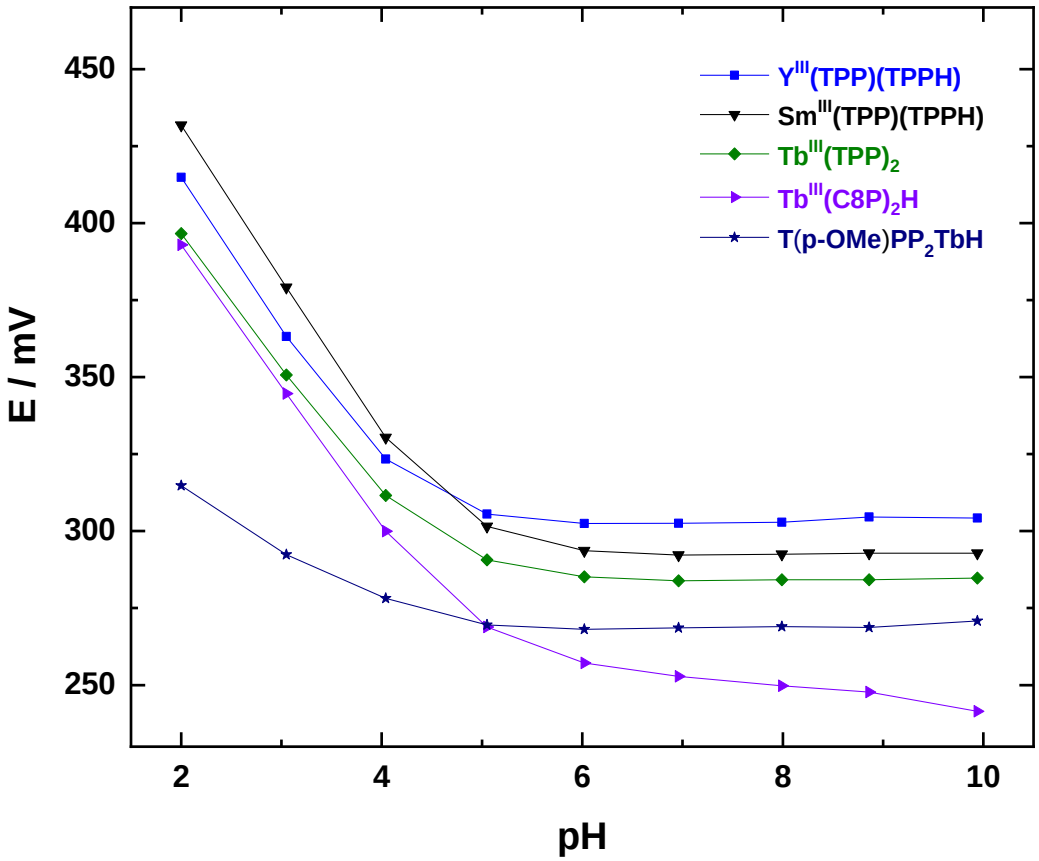

Figure 4: The pH sensitivity of porphyrin-based ISEs in 0.1 mol dm^{-3} KNO_3.

3.4. Density functional theory calculations.

Density functional theory (DFT) has been used in a number of ways to explore experimental potentiometric responses. These include simulation of energies of formation [33–36], frontier molecular orbitals [35], structures [37, 38], complex formation constants [39, 40] and spectroscopic characteristics [41, 42]. It has been used here to provide explanation of the cationic binding of the reported compounds (**Figure 2**). It was also used to simulate metal-binding energies (ΔE) which are presented in **Figures 5 and 6** and 'distortion energies' which are presented in supporting information, Figures S2. Definition of 'distortion energy' can be found in the experimental, and 'distortion energy' is illustrated in supporting information, Figure S1 for clarity. Both the aryl and porphyrin clefts were considered and were labeled accordingly. The functional (ωB97XD) and basis sets (Stuttgart ECP, LANL2DZ ECP and 6-31G(d,p)) were used as they have been shown to provide a satisfactory simulation of lanthanide double-decker porphyrins [15,27]. Attempts were made to simulate the yttrium, samarium and terbium structures of $M(TPP)_2$ and M(TPP)(HTPP), however only the yttrium structures were successfully optimized. For samarium and terbium convergence failures could not be resolved despite numerous attempts and the exploration of several ECP definitions. It remains unclear why these calculations failed, however it is presumed that this was related to issues with the definitions of electronic structure for the central element (i.e. yttrium vs samarium and terbium). No imaginary frequencies were returned for each optimized yttrium structure. A pictorial explanation of the computational procedure can be found in Figure S1. Experimental selectivity measurements for $Y(TPP)_2$ give the following selectivity coefficient patterns for silver over interfering ions, $\mathbf{Ag^+} > K^+ > Pb^{2+} > Cu^{2+} > Ni^{2+} > Co^{2+} > Cd^{2+} > Sr^{2+} > Na^+ > Zn^{2+} > Ca^{2+} > Mg^{2+}$. In this case Ag^+ is correctly identified as the most preferred metal cation (lowest ΔE) (**Figure 5**). Similar to the experimental results of selectivity, calculated ΔE values indicate the selectivity of the ISEs to silver over monovalent interfering ions followed the same pattern, namely $Ag^+ > K^+ > Na^+$ while the least interfering ions were found to be Zn^{2+}, Ca^{2+} and Mg^{2+}. On the other hand, calculated ΔE values were not highly consistent with the experimentally derived most interfering ions pattern (K^+, Cu^{2+}, Pb^{2+}), because DFT calculations indicated Na^+ as being the second most interfering ion. This could in part be attributed to sporadic variation for aryl and porphyrin cleft values. Interestingly, a large difference in energy was noted between the monovalent and divalent metals cations. For this reason, the ΔE values were considered separately. If only the aryl cleft was considered for divalent cations then there was some general trend with selectivity measurements, however the experimental selectivity

pattern was not exactly replicated by DFT calculations, e.g. Pb^{2+} was less 'preferable' than the experimental selectivity pattern indicated. If monovalent metal cations were considered, the difference between aryl and porphyrin cleft is smaller, e.g. Na^+ is correctly identified as the least preferred (highest ΔE) metal cation. Na^+ and K^+ energies provide a good example of the small differences (0.5 kJ mol^{-1}) between calculated ΔE values. This can be compared to a three magnitude difference of selectivity from experimental results.

Similar calculations were run for the Y(TPP)(HTPP) and are displayed in **Figure 6**. Experimental selectivity measurements for $Y(TPP)_2$ give the following selectivity coefficient patterns for silver over interfering ions, $\mathbf{Ag^+} > K^+ > Pb^{2+} > Cu^{2+} > Cd^{2+} > Co^{2+} > Na^+ > Ni^{2+} > Sr^{2+} > Zn^{2+} > Ca^{2+} > Mg^{2+}$. Yet again, similarly to the experimental results of selectivity, calculated ΔE values indicate the selectivity of the ISEs to silver over monovalent interfering ions followed the same pattern, namely $Ag^+ > K^+ > Na^+$ (Ag^+ gives the lowest ΔE and Na^+ gives the highest). On the contrary, the least interfering ions were found to be Zn^{2+}, Ni^{2+} and Mg^{2+} (Ca^{2+} being within uncertainty range of theoretical prediction). The divalent cations show somewhat of an agreement with selectivity trends in comparison to $Y(TPP)_2$ with some ions being 'outliers', e.g. Pb^{2+} was not the lowest energy, thus is not predicted to be the preferred ion. In **Figure 5**, ions were ordered with respect to r_{UAHF} radius. It does not appear that cation size and ΔE are correlated. To investigate the influence of cation size a 'distortion energy' was calculated (supporting information, Figure S1). This uses the structure of $MY(TPP)_2$ and removes the metal ion. A single point energy was run using this structure ($*Y(TPP)_2$) and the energy was compared to the optimized $Y(TPP)_2$ structure. Similar to ΔE values, the monovalent cation and divalent cation structures are somewhat different and are considered separately (supporting information, Figure S2). When considering Mg^{2+}, Ca^{2+}, Sr^{2+} and Pb^{2+} structures there is an increase of distortion energy with increasing r_{UAHF}. However, if the other divalent cations were considered (Zn^{2+}, Ni^{2+} and Cd^{2+}) this is no longer true. When considering the monovalent metals cations there is no apparent trend between distortion energy and r_{UAHF}. These results are the same when using $Y(TPP)_2$ and Y(TPP)(HTPP) structures (supporting information, Figures S2 a and b).

These DFT calculations showed some ability to predict selectivity of cations through ΔE. For example, Ag^+ is correctly predicted to be the most favored and Mg^{2+} is correctly predicted to be the least favored. However, the same magnitude or sensitivity for the potentiometric

measurements could not be replicated, e.g. there is a small separation between the ΔE, when selectivity values are several orders of magnitude different. DFT calculations are most applicable to small systems (generally less than 300 atoms) due to computational requirements. Thus, material influences on selectivity values, such as ion hydration energy and interactions between cations and the lipophilic anion and/or plasticizer in the membrane, are not considered by this *in vacuo* method. These can be especially relevant when the ion-ionophore complex is not very strong. Generally, DFT can provide sufficient description of chemical properties and bonding, especially when using crystallography structures as input [43, 44]. In this case, the ΔE calculations did not show good agreement with experiment, which could indicate that through space interactions of the host and guest were not well modeled or material properties need to be considered. The former explanation could be in part be due to poor description of the electronic structure by the 6-31G(d,p) basis set for this purpose, or a large basis set superposition error for this system [45].

Experimental complex formation constant (β) has been found to be directly related to the complex formation of ionophore with a target ion and therefore, has been used to provide information about the selectivities towards a given ion. To assess formation energies from the experimental complex formation constant (β), a constant phase-boundary potential is essential [39]. This was attempted also in this work. A buffered Ag^+ solution is required for the internal filling solution to keep the phase boundary potential constant. However, Ag^+ does not form a strong complex with e.g. EDTA ($\log \alpha_{Ag(EDTA)} = 1.5\text{-}2.6$; at pH 6-7) [46], which led to experimental difficulties and instability in the potentiometric response of the ISE. Therefore, the experimental determination of β using the method suggested in [39] was unsuccessful.

It is worth noting that a cation that is more strongly hydrated in the aqueous phase would be less eager to enter the hydrophobic membrane. For example, the Gibbs free energy of hydration [47] (ΔG_{hydr}) is –365 $kJmol^{-1}$ for Na^+ and –295 $kJmol^{-1}$ for K^+, which could explain why Na^+ interferes less than K^+ although their metal-binding energy is similar. Thus, theoretical predictions and experimental results of the ion-ionophore interactions may vary, however, DFT was found to be useful to predict the most selective ion for the porphyrin system as well as indicate initial selectivity patterns, which can be useful for screening for new ionophores.

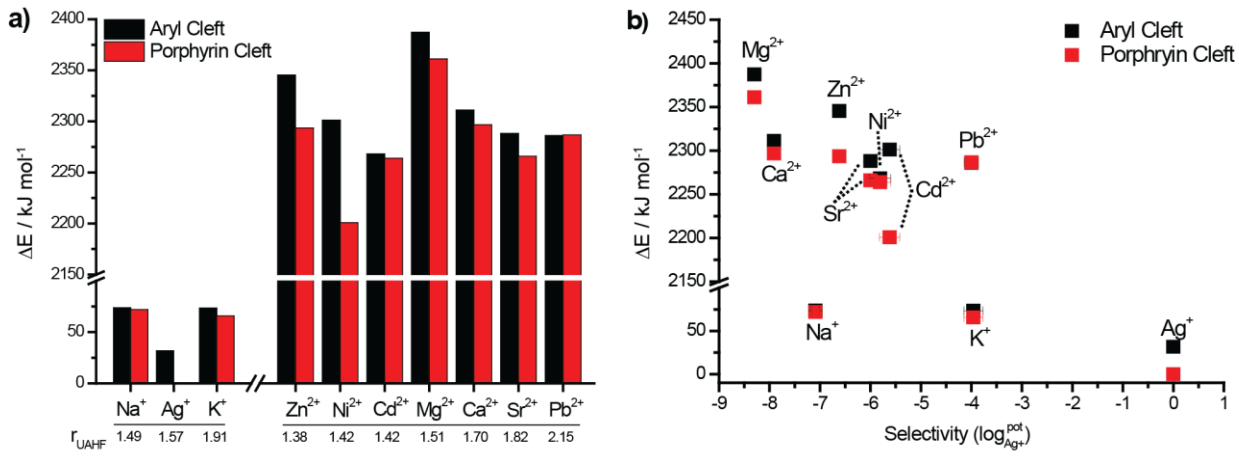

Figure 4. a) $Y(TPP)_2$ metal-binding energies (ΔE) relative to the lowest energy $Ag^{+}_{porphyin}$ structure and **b)** $Y(TPP)_2$ metal-binding energies (ΔE) relative to the lowest energy $Ag^{+}_{porphyin}$ structure vs $Y(TPP)_2$ electrochemical selectivity measurements.

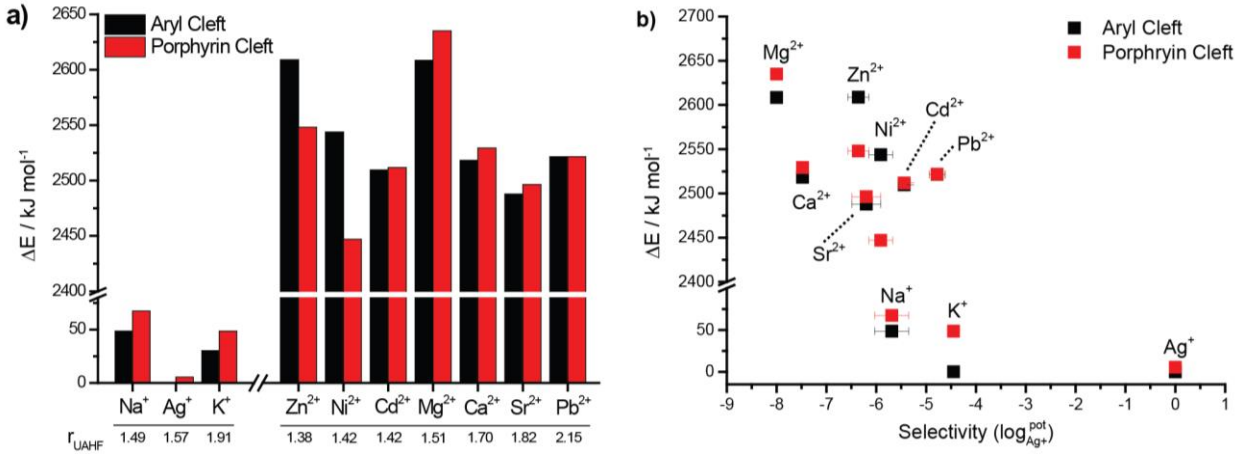

Figure 5. a) Y(TPP)(HTPP) metal-binding energies (ΔE) relative to the lowest energy $Ag^{+}_{porphyin}$ structure and **b)** Y(TPP)(HTPP) metal-binding energies (ΔE) relative to the lowest energy $Ag^{+}_{porphyin}$ structure vs Y(TPP)(HTPP) electrochemical selectivity measurements.

4. Conclusions

In this work the applicability of double-decker porphyrins were investigated for the use as ionophores in potentiometric ion sensors. All studied rare earth elements double-decker porphyrin based ISEs were found primarily selective to silver ions. Ion sensors based on non-protonated double-decker porphyrins containing terbium and yttrium, i.e. $Tb^{III}(TPP)_2$ and $Y^{III}(TPP)_2$, were

characterized with the best selectivity towards Ag^+ over other interfering ions. Experimentally obtained selectivity coefficients were compared to theoretical predictions based on DFT calculations of the metal-binding energies of complexes between double decker porphyrins ($Y^{III}(TPP)_2$ and $Y^{III}(TPP)(TPPH)$) and metal ions. The experimental selectivity pattern for monovalent ions ($Ag^+ > K^+ > Na^+$) agreed well with DFT calculations. Also, for all cases (experimental and calculated), the least interfering ions were found to be Zn^{2+}, Ca^{2+} and Mg^{2+} (Ni^{2+} instead of Ca^{2+} for $Y^{III}(TPP)(TPPH)$ based ISEs). The experimentally derived selectivity coefficients were found to carry a high uncertainty for some interfering cations that showed sub-Nernstian slopes. Furthermore, DFT calculations were performed *in vacuo* without taking into account some of the ion-solution and ion-membrane interactions. Nonetheless, DFT calculations are useful as a predictive tool to study various molecular systems for their possible selectivity and primary ion sensitivity when designing new ionophores for the use in ISEs.

Acknowledgements

This work is part of the activities of the Johan Gadolin Process Chemistry Centre at Åbo Akademi University. JEB thanks University of Otago for a PhD scholarship, Johan Gadolin Scholarship for financial support for his research visit to Laboratory of Analytical Chemistry at Åbo Akademi University and the New Zealand eScience Infrastructure (NeSI) for computational time. NKJ acknowledges financial support from K.H. Renlund's Foundation. KCG and JEB thank the MacDiarmid Institute for support. NKJ acknowledge GL acknowledges Academy of Finland (project number 295019) for financial support.

References

[1] P. Bühlmann, E. Pretsch, E. Bakker, Carrier-Based Ion-Selective Electrodes and Bulk Optodes. 2. Ionophores for Potentiometric and Optical Sensors., Chem. Rev. 98 (1998) 1593–1688. doi:10.1021/cr970113+.

[2] E. Bakker, P. Bühlmann, E. Pretsch, Carrier-Based Ion-Selective Electrodes and Bulk Optodes. 1. General Characteristics, Chem. Rev. 97 (1997) 3083–3132. doi:10.1021/cr940394a.

[3] N.K. Joon, N. He, T. Ruzgas, J. Bobacka, G. Lisak, PVC-based Ion-Selective Electrodes with a silicone rubber outer coating with improved analytical performance, Anal. Chem. (2019). doi:10.1021/acs.analchem.9b01490.

[4] B. Adhikari, S. Majumdar, Polymers in sensor applications, Prog. Polym. Sci. 29 (2004) 699–766. doi:10.1016/j.progpolymsci.2004.03.002.

[5] M. Biesaga, Porphyrins in analytical chemistry. A review, Talanta. 51 (2000) 209–224. doi:10.1016/S0039-9140(99)00291-X.

[6] R. Paolesse, D. Monti, S. Nardis, C. Di Natale, 54 Porphyrin-Based Chemical Sensors, in: 2011: pp. 121–225. doi:10.1142/9789814322386_0006.

[7] G. Lisak, T. Tamaki, T. Ogawa, Dualism of Sensitivity and Selectivity of Porphyrin Dimers in Electroanalysis, Anal. Chem. 89 (2017) 3943–3951. doi:10.1021/acs.analchem.6b04179.

[8] A.R. Fakhari, M. Shamsipur, K. Ghanbari, Zn(II)-selective membrane electrode based on tetra(2-aminophenyl) porphyrin, Anal. Chim. Acta. 460 (2002) 177–183. doi:10.1016/S0003-2670(02)00200-3.

[9] J.A. Schneider, J.F. Hornig, Spectrophotometric determination of lead in tap water with 5, 10, 15, 20-tetra (4-N-sulfoethylpyridinium)porphyrin using merging zones flow injection, Analyst. 118 (1993) 933–936. doi:10.1039/an9931800933.

[10] V.K. Gupta, A.K. Jain, L.P. Singh, U. Khurana, Porphyrins as carrier in PVC based membrane potentiometric sensors for nickel(II), Anal. Chim. Acta. 355 (1997) 33–41. doi:10.1016/S0003-2670(97)81609-1.

[11] P. Kumar, Y.-B. Shim, A novel Mg(II)-selective sensor based on 5,10,15,20-tetrakis(2-furyl)-21,23-dithiaporphyrin as an electroactive material, J. Electroanal. Chem. 661 (2011) 25–30.

doi:10.1016/j.jelechem.2011.07.005.

[12] Y.-Q. Weng, F. Yue, Y.-R. Zhong, B.-H. Ye, A Copper(II) Ion-Selective On−Off-Type Fluoroionophore Based on Zinc Porphyrin−Dipyridylamino, Inorg. Chem. 46 (2007) 7749–7755. doi:10.1021/ic061709v.

[13] V.K. Gupta, A.K. Jain, G. Maheshwari, H. Lang, Z. Ishtaiwi, Copper(II)-selective potentiometric sensors based on porphyrins in PVC matrix, Sensors Actuators B Chem. 117 (2006) 99–106. doi:10.1016/j.snb.2005.11.003.

[14] H.K. Lee, K. Song, H.R. Seo, Y.-K. Choi, S. Jeon, Lead(II)-selective electrodes based on tetrakis(2-hydroxy-1-naphthyl)porphyrins: the effect of atropisomers, Sensors Actuators B Chem. 99 (2004) 323–329. doi:10.1016/j.snb.2003.11.029.

[15] K. Yamashita, N. Sakata, T. Ogawa, Systematic Structural Elucidation for the Protonated Form of Rare Earth Bis(porphyrinato) Double-Decker Complexes: Direct Structural Evidence of the Location of the Attached Proton, Inorg. Chem. 55 (2016) 8935–8942. doi:10.1021/acs.inorgchem.6b01442.

[16] N.K. Joon, N. He, M. Wagner, M. Cárdenas, J. Bobacka, G. Lisak, Influence of phosphate buffer and proteins on the potentiometric response of a polymeric membrane-based solid-contact Pb(II) ion-selective electrode, Electrochim. Acta. 252 (2017) 490–497. doi:10.1016/j.electacta.2017.08.126.

[17] J. Bobacka, Potential Stability of All-Solid-State Ion-Selective Electrodes Using Conducting Polymers as Ion-to-Electron Transducers, Anal. Chem. 71 (1999) 4932–4937. doi:10.1021/ac990497z.

[18] E. Bakker, E. Pretsch, P. Bühlmann, Selectivity of Potentiometric Ion Sensors, Anal. Chem. 72 (2000) 1127–1133. doi:10.1021/ac991146n.

[19] E. Bakker, Determination of Unbiased Selectivity Coefficients of Neutral Carrier-Based Cation-Selective Electrodes, Anal. Chem. 69 (1997) 1061–1069. doi:10.1021/ac960891m.

[20] M. Dolg, H. Stoll, H. Preuss, R.M. Pitzer, Relativistic and correlation effects for element 105 (hahnium, Ha): a comparative study of M and MO (M = Nb, Ta, Ha) using energy-adjusted ab initio pseudopotentials, J. Phys. Chem. 97 (1993) 5852–5859. doi:10.1021/j100124a012.

[21] W.R. Wadt, P.J. Hay, Ab initio effective core potentials for molecular calculations. Potentials for

main group elements Na to Bi, J. Chem. Phys. 82 (1985) 284–298. doi:10.1063/1.448800.

[22] P.J. Hay, W.R. Wadt, Ab initio effective core potentials for molecular calculations. Potentials for K to Au including the outermost core orbitals, J. Chem. Phys. 82 (1985) 299–310. doi:10.1063/1.448975.

[23] T. H. Dunning Jr.and P. J. Hay, in Modern Theortical Chemistry, Ed. H. F. Schaefer III, 3 (1977) 1–28.

[24] P.C. Hariharan, J.A. Pople, The influence of polarization functions on molecular orbital hydrogenation energies, Theor. Chim. Acta. 28 (1973) 213–222. doi:10.1007/BF00533485.

[25] M.M. Francl, W.J. Pietro, W.J. Hehre, J.S. Binkley, M.S. Gordon, D.J. DeFrees, J.A. Pople, Self-consistent molecular orbital methods. XXIII. A polarization-type basis set for second-row elements, J. Chem. Phys. 77 (1982) 3654–3665. doi:10.1063/1.444267.

[26] M.J. Frisch, G.W. Trucks, H.B. Schlegel, G.E. Scuseria, M.A. Robb, J.R. Cheeseman, G. Scalmani, V. Barone, B. Mennucci, G.A. Petersson, Gaussian 09, revision A. 1, Gaussian Inc.Wallingford CT. 27 (2009).

[27] Y. Kitagawa, T. Kawakami, S. Yamanaka, M. Okumura, DFT and DFT-D studies on molecular structure of double-decker phthalocyaninato-terbium(III) complex, Mol. Phys. 112 (2014) 995–1001. doi:10.1080/00268976.2013.825341.

[28] M. Ikeda, M. Takeuchi, S. Shinkai, F. Tani, Y. Naruta, S. Sakamoto, K. Yamaguchi, Allosteric Binding of an Ag+ Ion to Cerium(IV) Bis-porphyrinates Enhances the Rotational Activity of Porphyrin Ligands, Chem. - A Eur. J. 8 (2002) 5541–5550. doi:10.1002/1521-3765(20021216)8:24<5541::AID-CHEM5541>3.0.CO;2-X.

[29] J. Bobacka, T. Lahtinen, J. Nordman, S. Häggström, K. Rissanen, A. Lewenstam, A. Ivaska, All-Solid-State Ag+-ISE Based on [2.2.2]p,p,p-Cyclophane, Electroanalysis. 13 (2001) 723–726. doi:10.1002/1521-4109(200105)13:8/9<723::AID-ELAN723>3.0.CO;2-R.

[30] M.M. Ardakani, H. Dehghani, M. Jalayer, H.R. Zare, Potentiometric determination of silver(I) by selective membrane electrode based on derivative of porphyrin, Anal. Sci. (2004). doi:10.2116/analsci.20.1667.

[31] X.B. Zhang, Z.X. Han, Z.H. Fang, G.L. Shen, R.Q. Yu, 5,10,15-Tris(pentafluorophenyl)corrole as highly selective neutral carrier for a silver ion-sensitive electrode, Anal. Chim. Acta. (2006).

doi:10.1016/j.aca.2006.01.056.

[32] D. Vlascici, E.F. Cosma, E.M. Pica, V. Cosma, O. Bizerea, G. Mihailescu, L. Olenic, Free base porphyrins as ionophores for heavy metal sensors, Sensors. (2008). doi:10.3390/s8084995.

[33] A.A. Abraham, M. Rezayi, N.S.A. Manan, L. Narimani, A.N. Bin Rosli, Y. Alias, A Novel Potentiometric Sensor Based on 1,2-Bis(N'-benzoylthioureido)benzene and Reduced Graphene Oxide for Determination of Lead (II) Cation in Raw Milk, Electrochim. Acta. 165 (2015) 221–231. doi:10.1016/j.electacta.2015.03.003.

[34] S. Riahi, M.F. Mousavi, S.Z. Bathaie, M. Shamsipur, A novel potentiometric sensor for selective determination of theophylline: Theoretical and practical investigations, Anal. Chim. Acta. 548 (2005) 192–198. doi:10.1016/j.aca.2005.05.074.

[35] M. Ghanei-Motlagh, M. Fayazi, M.A. Taher, On the potentiometric response of mercury(II) membrane sensors based on symmetrical thiourea derivatives—Experimental and theoretical approaches, Sensors Actuators B Chem. 199 (2014) 133–141. doi:10.1016/j.snb.2014.03.086.

[36] S. Demir, H. Yilmaz, M. Dilimulati, M. Andaç, An efficient ab initio DFT and PCM assessment of the potentiometric selectivity of a salophen type Schiff base, J. Mol. Model. 20 (2014) 2258(1–7). doi:10.1007/s00894-014-2258-9.

[37] M. Shamsipur, A.S. Dezaki, M. Akhond, H. Sharghi, Z. Paziraee, K. Alizadeh, Novel PVC-membrane potentiometric sensors based on a recently synthesized sulfur-containing macrocyclic diamide for Cd2 ion. Application to flow-injection potentiometry, J. Hazard. Mater. 172 (2009) 566–573. doi:https://doi.org/10.1016/j.jhazmat.2009.07.003.

[38] M. Shamsipur, M. Hosseini, K. Alizadeh, Z. Talebpour, M.F. Mousavi, M.R. Ganjali, M. Arca, V. Lippolis, PVC Membrane and Coated Graphite Potentiometric Sensors Based on Et 4 todit for Selective Determination of Samarium(III), Anal. Chem. 75 (2003) 5680–5686. doi:10.1021/ac0205659.

[39] A. Ceresa, E. Pretsch, Determination of formal complex formation constants of various Pb^{2+} ionophores in the sensor membrane phase, Anal. Chim. Acta. (1999). doi:10.1016/S0003-2670(99)00311-6.

[40] Y. Mi, E. Bakker, Determination of complex formation constants of lipophilic neutral ionophores in solvent polymeric membranes with segmented sandwich membranes, Anal. Chem. (1999).

doi:10.1021/ac9905930.

[41] H.J. Kim, S. Bhuniya, R.K. Mahajan, R. Puri, H. Liu, K.C. Ko, J.Y. Lee, J.S. Kim, Fluorescence turn-on sensors for HSO4−, Chem. Commun. (2009) 7128–7130. doi:10.1039/b918324h.

[42] B. Lakard, G. Herlem, M. Herlem, A. Etcheberry, J. Morvan, B. Fahys, Spectroscopic and ab initio study of polymeric films used as chemical sensors, Surf. Sci. 502–503 (2002) 296–303. doi:10.1016/S0039-6028(01)01967-7.

[43] D. Preston, J.E. Barnsley, K.C. Gordon, J.D. Crowley, Controlled Formation of Heteroleptic [Pd 2 (L a) 2 (L b) 2] 4+ Cages, J. Am. Chem. Soc. 138 (2016) 10578–10585. doi:10.1021/jacs.6b05629.

[44] J.E. Barnsley, G.E. Shillito, C.B. Larsen, H. van der Salm, L.E. Wang, N.T. Lucas, K.C. Gordon, Benzo[c][1,2,5]thiadiazole Donor–Acceptor Dyes: A Synthetic, Spectroscopic, and Computational Study, J. Phys. Chem. A. 120 (2016) 1853–1866. doi:10.1021/acs.jpca.6b00447.

[45] H.S. Choi, S.B. Suh, S.J. Cho, K.S. Kim, Ionophores and receptors using cation- interactions: Collarenes, Proc. Natl. Acad. Sci. 95 (1998) 12094–12099. doi:10.1073/pnas.95.21.12094.

[46] A. Ringbom, Complexation in Analytical Chemistry, Wiley-Interscinece. 16 (1963).

[47] Y. Marcus, Thermodynamics of solvation of ions. Part 5.—Gibbs free energy of hydration at 298.15 K, J. Chem. Soc., Faraday Trans. 87 (1991) 2995–2999. doi:10.1039/FT9918702995.